Available online at www.sciencedirect.com
SCIENCE DIRECT®
ELSEVIER
Nuclear Instruments and Methods in Physics Research B 227 (2005) 180–190
NIM B
Beam Interactions with Materials & Atoms
www.elsevier.com/locate/nimb

# Calculation of Smith–Purcell radiation from a volume strip grating

G. Kube *,[1]

*Deutsches Elektronen-Synchrotron DESY, Notkestrasse 85, D-22603 Hamburg, Germany*

Received 17 December 2003; received in revised form 12 February 2004

**Abstract**

Smith–Purcell radiation is generated by a charged particle beam passing close to the surface of a diffraction grating. Experimental investigations show a strong dependency of the emitted radiation intensity on the form of the grating profile. This influence is expressed by the radiation factor which is a measure of the grating efficiency, in close analogy to reflection coefficients of optical grating theories. The radiation factor depends on beam energy and observation geometry. Up to now calculations for radiation factors exist for lamellar, sinusoidal and échelette-type grating profiles. In this paper, calculations of Smith–Purcell radiation factors for volume strip gratings which are separated by vacuum gaps are presented. They are based on the modal expansion method and restricted to perfectly conducting grating surfaces and to electron trajectories perpendicular to the grating grooves. An infinite system of coupled linear algebraic equations for the scattered and the transmitted wave amplitudes is derived by imposing the continuity condition at the open end of the grooves, and by the boundary conditions at the remaining part of the interface. Numerical results are presented and discussed in view of using Smith–Purcell radiation for particle beam diagnostic purposes.


*PACS:* 41.60.−m; 42.25.Fx; 42.79.Dj
*Keywords:* Smith–Purcell radiation; Strip grating; Electron beam diagnostics

## 1. Introduction

The development of the next generation high quality electron beams presents an enormous challenge for both the diagnostic measurement of beam parameters and the accurate positioning and control of these beams. The currently used monitors are based on a number of different physical principles, and one technique is to use the radiation that can be produced by the beam itself. In this context nowadays beam diagnostics based on optical transition radiation is widely used [1–4]. However, the transition radiation technique entails the disadvantage of an interaction of the beam with the target leading to either the destruction of the high quality beam parameters or at high beam currents even of the screen. Hence the development of non-invasive, low cost, and compact beam monitors is demanded. Monitors based on synchrotron radiation, while non-invasive, are

* Tel.: +49-40-8998; fax: +49-40-8998-3077.
*E-mail address:* gero.kube@desy.de (G. Kube).
[1] Part of this work was carried out during the author's stay at the Institut für Kernphysik, Universität Mainz (Germany).

0168-583X/$ - see front matter © 2004 Elsevier B.V. All rights reserved.
doi:10.1016/j.nimb.2004.02.021

disadvantageous because they cannot be used in linear beam geometries. Another approach rather similar to the transition radiation technique is to exploit the radiation characteristics of diffraction radiation which is emitted when the electrons pass close to an obstacle [5–9]. In recent publications beam diagnostics based on resonant diffraction radiation is proposed which originates from electrons moving through an ideally conducting tilted target which is made by strips separated by vacuum gaps [10,11].

A rather similar and also non-destructive approach is to use Smith–Purcell (SP) radiation as a compact and inexpensive beam profile monitor. The radiation is generated when the electron beam passes a periodic structure like a diffraction grating at a fixed distance close to the surface. The radiation mechanism was predicted by Frank [12] and observed in the visible spectral range for the first time by Smith and Purcell [13] using a 250–300 keV electron beam.

Soon after the discovery of the SP effect also potential applications became topic of interest. The possibility to use coherent SP radiation as bunch length diagnostic was proposed in [14,15] and experimentally tested in Frascati [16]. SP radiation as high resolution position sensor was discussed in view of possible applications for ultra relativistic beam energies up to 500 GeV in [17]. The use of SP based imaging techniques for transverse beam diagnostics was experimentally verified at the 855 MeV electron beam of the Mainz Microtron MAMI [18].

One important conclusion from this experiment which is described in more detail in [19] is that the radiated power in the visible spectral region is very low which makes the usage of SP based beam diagnostics in the standard operation mode of an accelerator rather difficult. The measured intensity is in a satisfactory agreement with calculations based on the theory of Van den Berg which is formulated in close analogy to optical grating theories [20–22]. According to this approach the low intensity is a consequence of the extremely small radiation factors in the order of $|R_n|^2 \approx 10^{-5}, \ldots, 10^{-6}$ at 855 MeV for gratings with échelette-type profiles. The radiation factors strongly depend on the shape of the grating profile which was observed already in earlier experiments by Bachheimer [23]. Additionally they are a function of the beam energy and the observation geometry. Based on the approach of Van den Berg up to now calculations for radiation factors exist for lamellar, sinusoidal and échelette-type grating profiles. The main problem connected with this theory is that, in general, extensive numerical calculations are required until finally the numerical solution converges. A comprehensive comparison of the various calculation methods is summarized in [24]. Moreover, beside the experimental verification at ultra relativistic beam energies [19] the theory is well supported by experimental investigations of incoherent SP emission in the kiloelectron-volt range in the optical [25] and in the far-infrared spectral region [26].

Apart from the Van den Berg approach SP radiation is alternatively interpreted as caused by induced surface currents which arise when the beam electrons traverse the grating surface [27]. Based on this interpretation, in a recent publication the radiation factor for strip gratings was calculated [28]. For a grating with infinitely thin strips separated by vacuum gaps the radiation factor can be expressed by a simple analytical expression:

$$|R_n|^2 = \sin^2(n\pi a/D). \tag{1}$$

In this equation, $n$ denotes the diffraction order, $D$ the grating period and $a$ the vacuum gap spacing, cf. Fig. 1. As a consequence, for a proper choice of the grating parameters $a/D = \frac{1}{2}$ and odd-numbered diffraction orders $m = 2|n| + 1$, the radiation factor would amount $|R_m|^2 = 1$ independently on the beam energy. Furthermore, for $l = 2|n|$ the radiation factor $|R_l|^2$ would vanish resulting in a suppression of the even-numbered diffraction orders. With an intensity increase of the odd-numbered diffraction orders by 5–6 orders of magnitude in comparison to the experiment described in [19] SP radiation would be very attractive in view of particle beam diagnostics as pointed out in [18]. Unfortunately, calculations based on a surface current approach failed to predict the measured intensities by orders of magnitude at ultra relativistic beam energies [19].

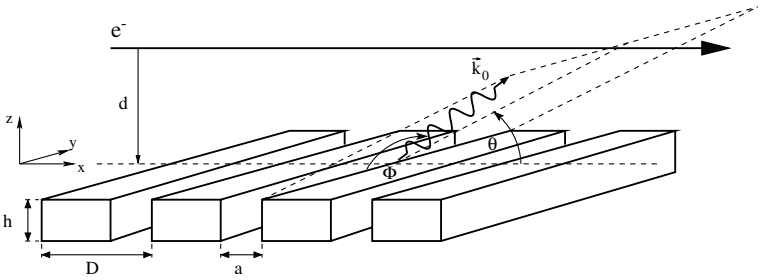


Fig. 1. Definition of the geometry. The electron moves with constant reduced velocity $\beta = v/c$ at a distance $d$ parallel to the grating surface in $x$-direction. The grooves of height $h$, oriented in the $y$-direction and separated by a vacuum gap $a$, repeat periodically with the grating period $D$. The direction of the photon wave vector $\vec{k}_0$ is described in the emission plane resulting from the $z = 0$ plane by a rotation about the $y$-axis by the angle $\theta$. In the emission plane the $\vec{k}_0$ vector makes an angle $\Phi$ with the $y$-axis.

In this article calculations of SP radiation factors for a strip grating are considered which are based on the theory of Van den Berg. The formalism of the theory is applied to the case of a strip grating with finite strip height $h$ (volume strip grating) whose strips are separated by vacuum gaps. For this geometry it is possible to use the modal expansion method which for lamellar grating profiles has been developed by Van den Berg [22] based on the treatment of Deryugin [29] for the case of $H$ polarization, i.e. the vector of the electric field is oriented perpendicular to the grating grooves. Later on it has been generalized by Haeberlé to both polarization states [30]. Following this method, infinite systems of coupled linear algebraic equations for the scattered and the transmitted wave amplitudes for both polarization states are derived. The systems are solved by the method of truncation and the results for the calculated radiation factors are discussed in view of applying SP radiation for both longitudinal and transverse beam diagnostics.

## 2. Smith–Purcell radiation properties

In this section a short summary of the main properties of SP radiation is given. According to the theory of di Francia [31], the emission mechanism of SP radiation can be interpreted in analogy to the diffraction of light as the diffraction of the field of the electrons (virtual photons) which pass the grating at a distance $d$ away from its surface by the grating grooves. One characteristic signature of SP radiation is that it must fulfill the dispersion relation [13]

$$\lambda = \frac{D}{|n|}(1/\beta - \cos\theta \sin\Phi). \tag{2}$$

In this equation $\lambda$ is the wavelength of the emitted radiation, $D$ the grating period, $n$ the diffraction order, $\beta = v/c$ the reduced electron velocity and $\theta$, $\Phi$ the emission angles as introduced in Fig. 1.

The angular distribution of the emitted power radiated into the $n$th order reads [31]

$$\frac{\mathrm{d}P_n}{\mathrm{d}\Omega} = \frac{eIn^2L}{2D^2\varepsilon_0}\frac{\sin^2\theta\sin^2\Phi}{(1/\beta - \cos\theta\sin\Phi)^3}|R_n|^2 \times \exp\left(-\frac{d}{h_{\mathrm{int}}}\sqrt{1+(\beta\gamma\cos\Phi)^2}\right), \tag{3}$$

with $e$ the elementary charge, $I$ the beam current, $L$ the grating length, $\varepsilon_0$ the vacuum permittivity and $d$ the distance of the beam above the grating. The calculation of the radiation factors $|R_n|^2$ is outlined in the subsequent section for the case of a perfectly conducting volume strip grating.

According to Eq. (3) the intensity decreases exponentially with increasing distance $d$ between electron beam and grating surface. The interaction length

$$h_{\mathrm{int}} = \frac{\lambda\beta\gamma}{4\pi}, \tag{4}$$

where $\gamma = (1-\beta^2)^{-1/2}$ is the Lorentz factor, describes the characteristic finite range of the virtual photons emitted and re-absorbed by the electrons.

Furthermore, at ultra relativistic electron energies, according to Eq. (3) the radiation is emitted in a very narrow angular region around $\Phi = 90°$, i.e. in the plane containing the grating normal and the electron beam. For ultra relativistic beam energies the characteristic opening angle (FWHM) can be written as

$$\Delta\Phi = 2\sqrt{\left(\frac{\ln 2}{4\pi}\frac{\lambda}{d}\right)^2 + \frac{1}{\beta\gamma}\frac{\ln 2}{2\pi}\frac{\lambda}{d}}, \tag{5}$$

i.e. the angular width can be controlled by the beam energy, the wavelength of observation and the distance between beam and grating surface. As described in [18] the feature of the strongly collimated emission can be exploited for SP based imaging techniques in the case of transverse beam diagnostics.

## 3. Radiation factors

In the following a short outline of the underlying ideas is given which leads to the derivation of the infinite systems of coupled linear algebraic equations. For a detailed description of the Van den Berg theory which is the basis for the subsequent considerations the reader is referred to [20–22,24].

In Figs. 1 and 2 a schematical description of the relevant quantities is shown. The electron moves in vacuum with constant reduced velocity $\beta = v/c$ in $x$-direction parallel to the grating surface along the trajectory $y = 0$, $z = z_0 = d + h/2 = \text{const}$. Top and bottom surface of the grating are located in the $(x, y)$-plane at $z_{\max} = +h/2$ respectively $z_{\min} = -h/2$.

According to Van den Berg the electric and magnetic field vectors of the incoming particle Coulomb field and the outgoing scattered fields are expanded in Fourier integrals with respect to time $t$ and $y$ coordinate. The $x$ and $z$ components of the Fourier transforms can be expressed as functions of the $y$ components of the field vectors which satisfy two-dimensional Helmholtz equations. Therefore only the $y$ components are considered in the following. By imposing the continuity condition at the open ends of the grooves and the boundary condition at the remaining parts of the interface, the infinite systems of linear equations for the amplitudes of the reflected and the transmitted fields are derived. For this purpose the fields in regions (I)–(III) according to Fig. 2 has to be specified.

The solution of the Helmholtz equations in the half space above the grating ($z \geqslant +h/2$) is composed by two contributions: the inhomogeneous solution which represents the incoming particle field described by an evanescent plane wave, and the homogeneous solution for the reflected wave amplitudes which is represented by a Rayleigh expansion:

$$E_y(x, z; \eta, \omega) = E_0 e^{i\alpha_0 x} e^{-|\gamma_0||z - z_0|} + \sum_{n=-\infty}^{\infty} E^{\mathrm{I}}_{y,n}(\eta, \omega) e^{i(\alpha_n x + \gamma_n z)}, \tag{6}$$

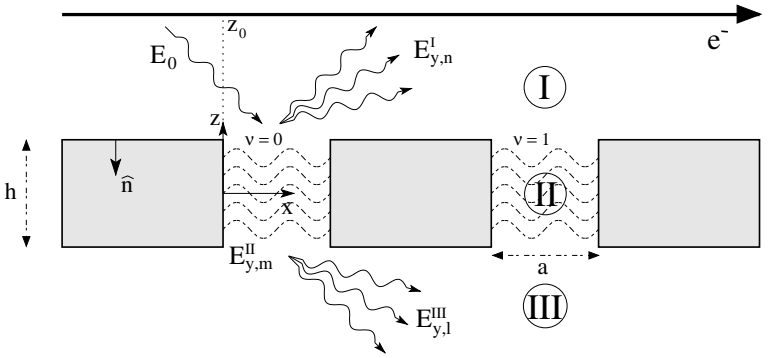


Fig. 2. Geometry of the volume strip grating. As example the electric fields in the various regions (I)–(III) are illustrated. $v$ denotes the index of the local $x$ coordinate inside the grating grooves.

$$H_y(x,z;\eta,\omega) = H_0 e^{i\alpha_0 x} e^{-|\gamma_0||z-z_0|} + \sum_{n=-\infty}^{\infty} H^{I}_{y,n}(\eta,\omega) e^{i(\alpha_n x+\gamma_n z)}. \quad (7)$$

In these equations, $\alpha_0 = \omega/v = k_0 c/v$ is the longitudinal component and $\eta$ respectively $\gamma_0 = i(\alpha_0^2+\eta^2-k_0^2)^{1/2}$ are the transversal components of the incoming wave with wave number $k_0$. According to Fig. 1 the corresponding components of the scattered waves are expressed by the angles of emergence as $\alpha_n = k_0 \sin\Phi\cos\theta$, $\eta = k_0\cos\Phi$ and $\gamma_n = k_0 \sin\Phi\sin\theta$. The amplitudes of the incoming field are $E_0 = q/2(\mu_0/\varepsilon_0)^{1/2} \times (\eta/k_0)(\alpha_0/\gamma_0)$ respectively $H_0 = -q/2\mathrm{sgn}(z-z_0)$ with $q$ the electron charge [21].

Inside the grating grooves (i.e. $-h/2 \leqslant z \leqslant +h/2$ and $0 < x_v < a$) the solution of the Helmholtz equation is expressed by a series of cavity modes. Following [32] the modal expansion can be written as

$$E_y(x,z;\eta,\omega) = \exp(i\alpha_0 vD) \times \sum_{m=-\infty}^{\infty} \left[ E^{II'}_{y,m}(\eta,\omega) e^{-i\kappa_m z} \sin(m\pi x_v/a) + E^{II''}_{y,m}(\eta,\omega) e^{+i\kappa_m z} \sin(m\pi x_v/a) \right], \quad (8)$$

$$H_y(x,z;\eta,\omega) = \exp(i\alpha_0 vD) \times \sum_{m=-\infty}^{\infty} \left[ H^{II'}_{y,m}(\eta,\omega) e^{-i\kappa_m z} \cos(m\pi x_v/a) + H^{II''}_{y,m}(\eta,\omega) e^{+i\kappa_m z} \cos(m\pi x_v/a) \right] \quad (9)$$

with $x_v$ the local $x$ coordinate in the $v$th groove (i.e. $x = vD + x_v$ with $v = 0, \pm1, \pm2, \ldots$) and $\kappa_m = \{k_0^2 - \eta^2 - (m\pi/a)^2\}^{1/2}$.

The solution of the homogeneous Helmholtz equation in the half space below the grating ($z \leqslant -h/2$) is represented again by a Rayleigh expansion,

$$E_y(x,z;\eta,\omega) = \sum_{l=-\infty}^{\infty} E^{III}_{y,l}(\eta,\omega) e^{i(\alpha_l x-\gamma_l z)}, \quad (10)$$

$$H_y(x,z;\eta,\omega) = \sum_{l=-\infty}^{\infty} H^{III}_{y,l}(\eta,\omega) e^{i(\alpha_l x-\gamma_l z)}. \quad (11)$$

The radiation factor is determined by the amplitudes of the outgoing reflected fields, i.e. by $E^{I}_{y,n}$ and $H^{I}_{y,n}$. According to [21] the following relations hold:

$$|R_n|^2 = \frac{4}{q^2}\exp[2|\gamma_0|(z_0-h/2)] \times \left\{ \frac{\varepsilon_0}{\mu_0} E^{I}_{y,n} E^{I*}_{y,n} + H^{I}_{y,n} H^{I*}_{y,n} \right\} \frac{k_0^2}{k_0^2-\eta^2} \quad (12)$$

$$= \{ \overline{E}^{I}_{y,n} \overline{E}^{I*}_{y,n} + \overline{H}^{I}_{y,n} \overline{H}^{I*}_{y,n} \} \frac{k_0^2}{k_0^2-\eta^2}, \quad (13)$$

with

$$\overline{E}^{I}_{y,n} = \sqrt{\frac{\varepsilon_0}{\mu_0}}\frac{2}{q}\exp[|\gamma_0|(z_0-h/2)] E^{I}_{y,n}, \quad (14)$$

$$\overline{H}^{I}_{y,n} = \frac{2}{q}\exp[|\gamma_0|(z_0-h/2)] H^{I}_{y,n}. \quad (15)$$

In a similar way it is possible to define a transmission factor for the amplitudes of the transmitted field component:

$$|T_n|^2 = \left\{ \overline{E}^{III}_{y,n} \overline{E}^{III*}_{y,n} + \overline{H}^{III}_{y,n} \overline{H}^{III*}_{y,n} \right\} \frac{k_0^2}{k_0^2-\eta^2}. \quad (16)$$

The task is to derive relations by which the reduced amplitudes $\overline{E}_{y,n}$, $\overline{H}_{y,n}$ in the region (I) above respectively (III) below the grating can be obtained. In this case according to Eqs. (13) and (16) it is possible to determine the radiation respectively the transmission factors by which the emitted power Eq. (3) can be calculated. For this purpose the continuity condition at the open end of the grooves ($0 < x < a$)

$$\lim_{z\downarrow\pm h/2} U_y = \lim_{z\uparrow\pm h/2} U_y, \qquad \lim_{z\downarrow\pm h/2} \partial_z U_y = \lim_{z\uparrow\pm h/2} \partial_z U_y, \quad (17)$$

with $U_y(x,z;\eta,\omega)$ the electric respectively magnetic field has to be exploited together with the boundary conditions for the fields on the ridges ($a < x_v < D$)

$$E_y(x_v, \pm h/2;\eta,\omega) = 0, \qquad \hat{n}\cdot\nabla H_y(x_v,\pm h/2;\eta,\omega) = 0, \quad (18)$$

where $\hat{n}$ denotes the unit vector normal to the grating surface, cf. Fig. 2. By means of these conditions the field amplitudes in the various regions (I)–(III) can be connected together.

### 3.1. Determination of $\overline{H}_y$

Inserting the combination of Eqs. (7) and (9) at the boundary I/II and the combination of Eqs. (9) and (11) at the boundary II/III into Eqs. (17) and (18) results in two equations for $H^{\mathrm{II}'}_{y,m}$ and $H^{\mathrm{II}''}_{y,m}$. This allows to get rid of these two coefficients of the modal expansion and to obtain a coupled system of linear equations involving only the coefficients $H^{\mathrm{I}}_{y,n}$, $H^{\mathrm{III}}_{y,n}$ of the Rayleigh expansion needed to calculate the radiation factor Eq. (13) respectively the transmission factor Eq. (16). This system for the reduced amplitudes of the magnetic field reads

$$\sum_{n=-\infty}^{\infty}[\gamma_n D\delta_{k,n}-V_{k,n}]\mathrm{e}^{\mathrm{i}\gamma_n h/2}\overline{H}^{\mathrm{I}}_{y,n}+\sum_{n=-\infty}^{\infty}B_{k,n}\mathrm{e}^{\mathrm{i}\gamma_n h/2}\overline{H}^{\mathrm{III}}_{y,n}=C^{\mathrm{I}}_k, \tag{19}$$

$$\sum_{n=-\infty}^{\infty}B_{k,n}\mathrm{e}^{\mathrm{i}\gamma_n h/2}\overline{H}^{\mathrm{I}}_{y,n}+\sum_{n=-\infty}^{\infty}[\gamma_n D\delta_{k,n}-V_{k,n}]\mathrm{e}^{\mathrm{i}\gamma_n h/2}\overline{H}^{\mathrm{III}}_{y,n}=C^{\mathrm{III}}_k,$$

with $k=0,\pm1,\pm2,\ldots$ In Eq. (19) the quantities are defined as follows:

$$C^{\mathrm{I}}_k=\gamma_0 D\delta_{k,0}+a\sum_{m=0}^{\infty}\varepsilon_m\kappa_m\frac{\Gamma_m+1}{\Gamma_m-1}\Psi_{m,k}\Psi^*_{m,0}, \tag{20}$$

$$C^{\mathrm{III}}_k=-2a\sum_{m=0}^{\infty}\varepsilon_m\kappa_m\frac{\mathrm{e}^{\mathrm{i}\kappa_m h}}{\Gamma_m-1}\Psi_{m,k}\Psi^*_{m,0}, \tag{21}$$

$$V_{k,n}=a\sum_{m=0}^{\infty}\varepsilon_m\kappa_m\frac{\Gamma_m+1}{\Gamma_m-1}\Psi_{m,k}\Psi^*_{m,n}, \tag{22}$$

$$B_{k,n}=2a\sum_{m=0}^{\infty}\varepsilon_m\kappa_m\frac{\mathrm{e}^{\mathrm{i}\kappa_m h}}{\Gamma_m-1}\Psi_{m,k}\Psi^*_{m,n}, \tag{23}$$

$$\Psi_{m,n}=a^{-1}\int_0^a \mathrm{d}x\cos(m\pi x/a)\exp(-\mathrm{i}\alpha_n x), \tag{24}$$

$$\Gamma_m=\exp(2\mathrm{i}\kappa_m h), \tag{25}$$

$$\varepsilon_m=2-\delta_{m,0}. \tag{26}$$

### 3.2. Determination of $\overline{E}_y$

The analogous procedure, applied to the electric fields Eqs. (6) and (8) at the boundary I/II and Eqs. (8) and (10) at the boundary II/III, leads to the coupled system of linear equations for the reduced amplitudes of the electric field,

$$\sum_{n=-\infty}^{\infty}[-D\delta_{k,n}+\gamma_n V_{k,n}]\mathrm{e}^{\mathrm{i}\gamma_n h/2}\overline{E}^{\mathrm{I}}_{y,n}+\sum_{n=-\infty}^{\infty}\gamma_n B_{k,n}\mathrm{e}^{\mathrm{i}\gamma_n h/2}\overline{E}^{\mathrm{III}}_{y,n}=C^{\mathrm{I}}_k, \tag{27}$$

$$\sum_{n=-\infty}^{\infty}\gamma_n B_{k,n}\mathrm{e}^{\mathrm{i}\gamma_n h/2}\overline{E}^{\mathrm{I}}_{y,n}+\sum_{n=-\infty}^{\infty}[-D\delta_{k,n}+\gamma_n V_{k,n}]\mathrm{e}^{\mathrm{i}\gamma_n h/2}\overline{E}^{\mathrm{III}}_{y,n}=C^{\mathrm{III}}_k,$$

with $k=0,\pm1,\pm2,\ldots$ and

$$C^{\mathrm{I}}_k=\frac{\eta}{k_0}\frac{\alpha_0}{\gamma_0}\left[D\delta_{k,0}+2a\gamma_0\sum_{m=1}^{\infty}\frac{\Gamma_m+1}{\kappa_m(\Gamma_m-1)}\Phi_{m,k}\Phi^*_{m,0}\right], \tag{28}$$

$$C^{\mathrm{III}}_k=4a\frac{\eta}{k_0}\alpha_0\sum_{m=1}^{\infty}\frac{\mathrm{e}^{\mathrm{i}\kappa_m h}}{\kappa_m(\Gamma_m-1)}\Phi_{m,k}\Phi^*_{m,0}, \tag{29}$$

$$V_{k,n}=2a\sum_{m=1}^{\infty}\frac{\Gamma_m+1}{\kappa_m(\Gamma_m-1)}\Phi_{m,k}\Phi^*_{m,n}, \tag{30}$$

$$B_{k,n}=4a\sum_{m=1}^{\infty}\frac{\mathrm{e}^{\mathrm{i}\kappa_m h}}{\kappa_m(\Gamma_m-1)}\Phi_{m,k}\Phi^*_{m,n}, \tag{31}$$

$$\Phi_{m,n}=a^{-1}\int_0^a \mathrm{d}x\sin(m\pi x/a)\exp(-\mathrm{i}\alpha_n x). \tag{32}$$

For the determination of the reflected and transmitted fields the infinite systems of equations are truncated and the order of truncation $N$ is increased until convergence is achieved. Eqs. (19) respectively (27) represent a $(4N+2)$ dimensional system of linear coupled equations. The coefficients of this matrix system can be calculated analytically, and the solution for all different modes is directly obtained by inversion of the matrix.

## 4. Numerical results

In the following computational results are presented for radiation and transmission factors at ultra relativistic energies. In this case SP radiation

is emitted under $\Phi = 90°$, cf. Eq. (5) and the incoming electric field vanishes because $E_0 = 0$. Due to the boundary conditions at the grating surface also the reflected electric field equals zero, therefore the calculation of $|R_n|^2$, $|T_n|^2$ is restricted to the determination of the magnetic field Eq. (19).

In order to achieve a sufficient accuracy at the one hand and a reasonable computational time at the other hand for the subsequent calculations the order of truncation is chosen as $N = 100$. Compared to a calculation with $N = 500$ the change in $|R_n|^2$ and $|T_n|^2$ due to the truncation is less than 5%. Furtheron in order to obtain reliable convergence of the numerical solution by reducing the number of propagating diffraction orders the lower limit in $\lambda/D$ is chosen as 0.2.

In Fig. 3 radiation and transmission factors are shown as function of the ratio $\lambda/D$ for various aspect ratios $h/D$ and $a/D = 0.5$, $|n| = 1$ and $E = 855$ MeV which corresponds to the beam energy of the experiment reported in [19]. In these figures, the most striking feature is the occurrence of sharp fluctuations at some critical values of $\lambda/D$ which are more pronounced for higher aspect ratios $h/D$. A number of fluctuations is related to the Wood–Rayleigh anomalies [33] and occurs at values of $\lambda/D$ at which an evanescent reflected respectively transmitted wave changes into a propagating one. The remaining fluctuations correspond to values of $\lambda/D$ at which an evanescent mode in the grating grooves changes into a propagating one [22].

From Fig. 3 it can be concluded that $|R_1|^2 \ll 1$ for the volume strip grating at 855 MeV, although the ratio $a/D = \frac{1}{2}$ was chosen such that $|R_1|^2 = 1$ according to Eq. (1). At ultra relativistic beam

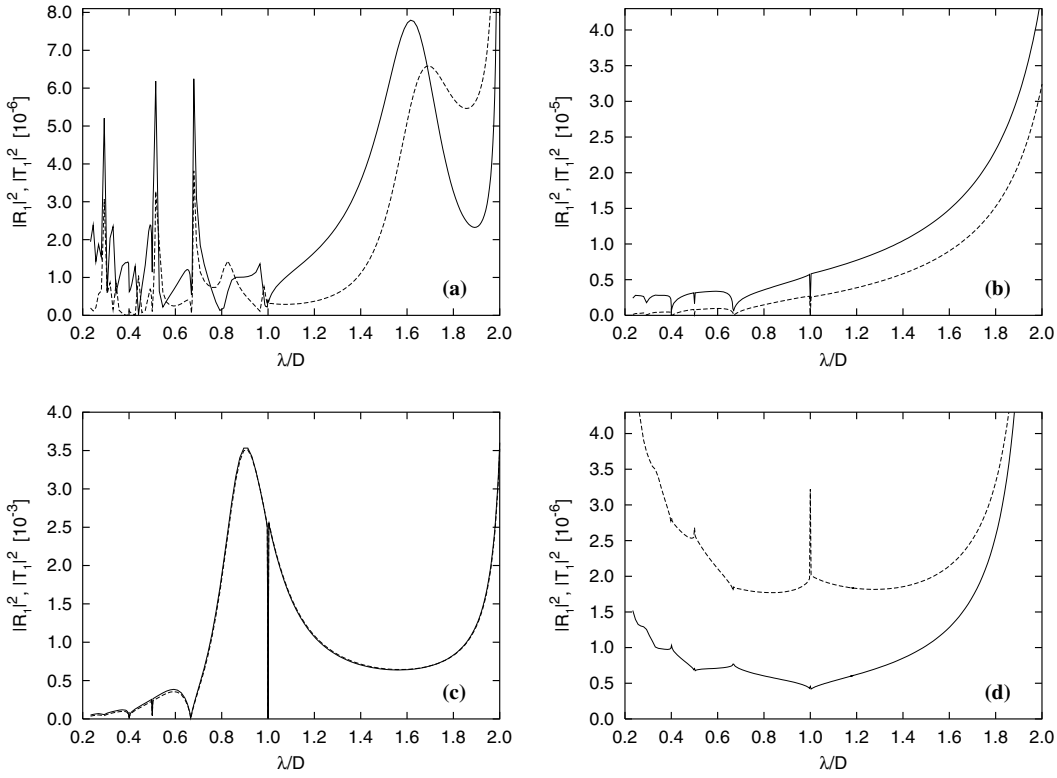


Fig. 3. Calculated functional dependence of radiation factors (solid line) and transmission factors (dashed line) on the ratio $\lambda/D$ for $h/D = 1$ (a), 0.1 (b), 0.01 (c) and 0.001 (d). Parameters of calculation: $a/D = 0.5$, $|n| = 1$ and $E = 855$ MeV. Note the different scaling factors of the ordinates.

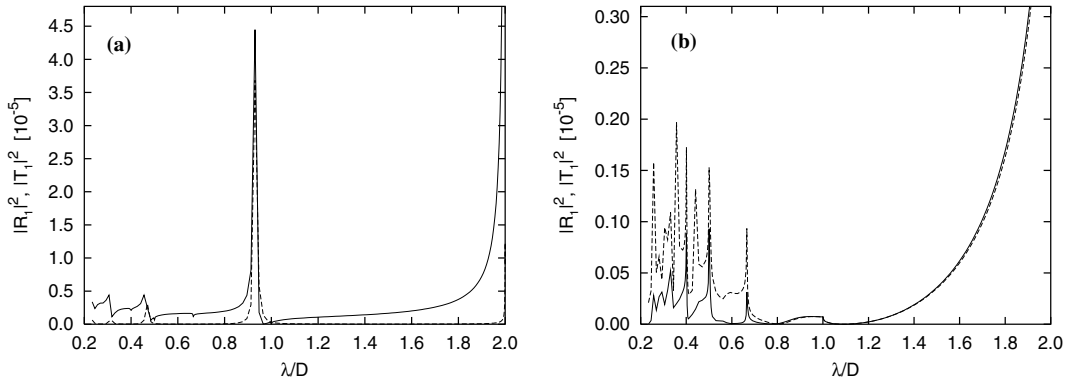


Fig. 4. Radiation factors (solid line) and transmission factors (dashed line) as function of $\lambda/D$ for $a/D = 0.1$ (a) and 0.9 (b). Parameters of calculation: $h/D = 0.5$, $|n| = 1$ and $E = 855$ MeV.

energies the calculations based on the Van den Berg theory are therefore in contradiction to the ones of the surface current model, a fact which was pointed out already for échelette-type grating profiles in [19]. Additionally it is alluded that the radiation factors for the volume strip grating in second diffraction order do not vanish as expected from Eq. (1) for $a/D = \frac{1}{2}$.

In Fig. 4 calculations are shown with the ratio $a/D$ as parameter and $h/D = 0.5$, $|n| = 1$ and $E = 855$ MeV. From these two examples it can be seen that a variation in a/D influences the shape of the anomalies drastically, but it does not result in a significant increase of $|R_1|^2$, $|T_1|^2$.

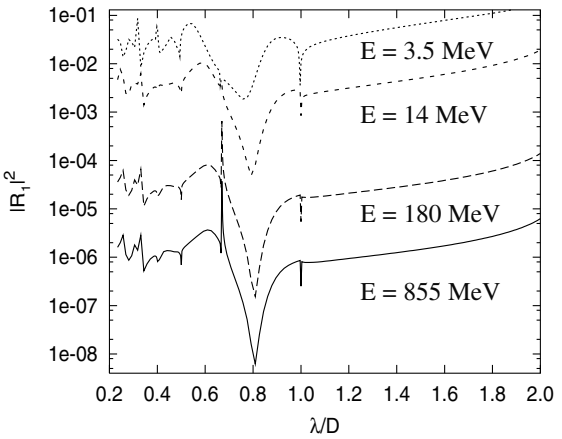


Fig. 5. Calculated functional dependence of the radiation factor $|R_1|^2$ on the ratio $\lambda/D$ for various electron energies. Parameters of grating: $a/D = 0.5$, $h/D = 0.495$.

The energy dependence of the radiation factors is calculated in Fig. 5. They scale roughly inversely proportional to $\gamma^2$ in contradiction to the predictions of a constant behavior from the surface current model in [28]. This dependency was pointed out already in [19] for échelette-type grating profiles. The strong energy dependence can be illustrated by a simple picture: in the limiting case $\beta \to 1$ the incoming virtual photon field with characteristic opening angle $1/\gamma$ transforms in a real one which propagates parallel to the grating surface, i.e. the photons are not diffracted and the radiation factor equals zero. Nevertheless a well-founded explanation for the $\gamma^{-2}$ decrease found empirically is still due.

## 5. Smith–Purcell radiation and beam diagnostics

Based on the preceding calculations this section is devoted to the usage of SP radiation in view of particle beam diagnostics. As indicated in this article the use of a strip grating profile for the radiation generation does not help offhand to overcome the problems of SP based diagnostics which are discussed in detail in [18]. In any case a careful optimization of the grating for the specific purpose of application has to be done.

In the case of transverse beam diagnostics the limiting factor for SP based beam imaging is the

extremely low radiated intensity. As can be seen from Fig. 3(c) where $|R_1|^2$ is in the order of $10^{-3}$ it is possible to increase the radiation factor in comparison to the experiment reported in [18,19]. This increase by about three orders of magnitude at $E = 855$ MeV could help to establish SP radiation as diagnostic tool. According to this example with $h/D = 0.01$, a typical wavelength $\lambda = 500$ nm in the optical spectral region and the maximum of the radiation factor at $\lambda/D \approx 0.9$, the grating parameters would be $D \approx 555.6$ nm respectively $h \approx 5.6$ nm. The technical realization of such a grating with self-supporting strips in the nanometer region separated by vacuum gaps seems to be unrealistic. Therefore more detailed optimization studies are required taking into account in addition the technical aspects.

A possibility to elude this problem is to work at longer wavelengths. According to Eq. (5) this could be done without affecting the strongly collimated emission in $\Phi$ if the distance $d$ between electron beam and grating surface is scaled simultaneously. However, an increase in the wavelength results in a decrease in the radiated power as can be seen if the dispersion relation Eq. (2) is inserted in Eq. (3). Additionally it has to be taken into account that detector systems in the infrared or even far-infrared spectral region are less sensitive than at optical wavelengths. As a result the increase in the radiation factor could be canceled out by the decrease of the emitted power and the detection efficiency.

As an alternative it might also be considered to build up the grating from a substrate covered by thin metal strips. However, this approach would require a modified theory which takes into account the modification of the modal expansion due to the material properties of the substrate and is out of the scope of this article.

The longitudinal beam diagnostics for bunch length determination is based on the investigation of the coherently emitted power as function of the wavelength. For SP radiation this corresponds to a measurement of the intensity as function of the observation angle $\theta$ due to the dispersion relation Eq. (2). As pointed out in [18] in this case the limiting factor is the angular respectively $\lambda/D$ dependence of the radiation factors which may destroy the signature on the bunch leading to a misinterpretation of bunch shape and length.

From Fig. 3 it is to conclude that the influence of the anomalies is weaker for shallow gratings. At least the fluctuations which arise due to the transformation of an evanescent mode in the grating grooves into a propagating one are less pronounced and finally disappear in the limiting case $h \to 0$. This effect of "smoothing out" is not only a property of a strip grating as indicated in Fig. 6 where additional calculations for lamellar and échelette-type profiles are shown. Therefore bunch lengths measurements with SP radiation based on the radiation production from shallow gratings might be a promising approach. In this case even the restriction due to the technical constraints is less severe because the region where the transition from incoherent to coherent radiation emission occurs is typically in the far-infrared spectral range.

## 6. Summary

In the present article a model for the determination of radiation and transmission factors for Smith–Purcell radiation from a volume strip grating together with numerical calculations are presented. The calculated values of $|R_1|^2$, $|T_1|^2$ strongly depend on the beam energy and are in the order of $10^{-6}$ at 855 MeV in accordance with the radiation factors for échelette-type grating profiles and the experimental findings of [19]. The calculations based on this model show large deviations in comparison to the radiation factor Eq. (1) as expected from the surface current model [27,28]. In this context one has to consider two main differences in the underlying approaches.

First the surface current model belongs to the category of scalar grating theories in which no polarization effects are included which are responsible for the appearance of Wood–Rayleigh anomalies. This simplification was already pointed out in [27]. Falling back to experimental verifications of optical grating theories which are the basis of the Van den Berg theory it is known that there was often poor agreement between scalar models and experiments. For a detailed discussion the

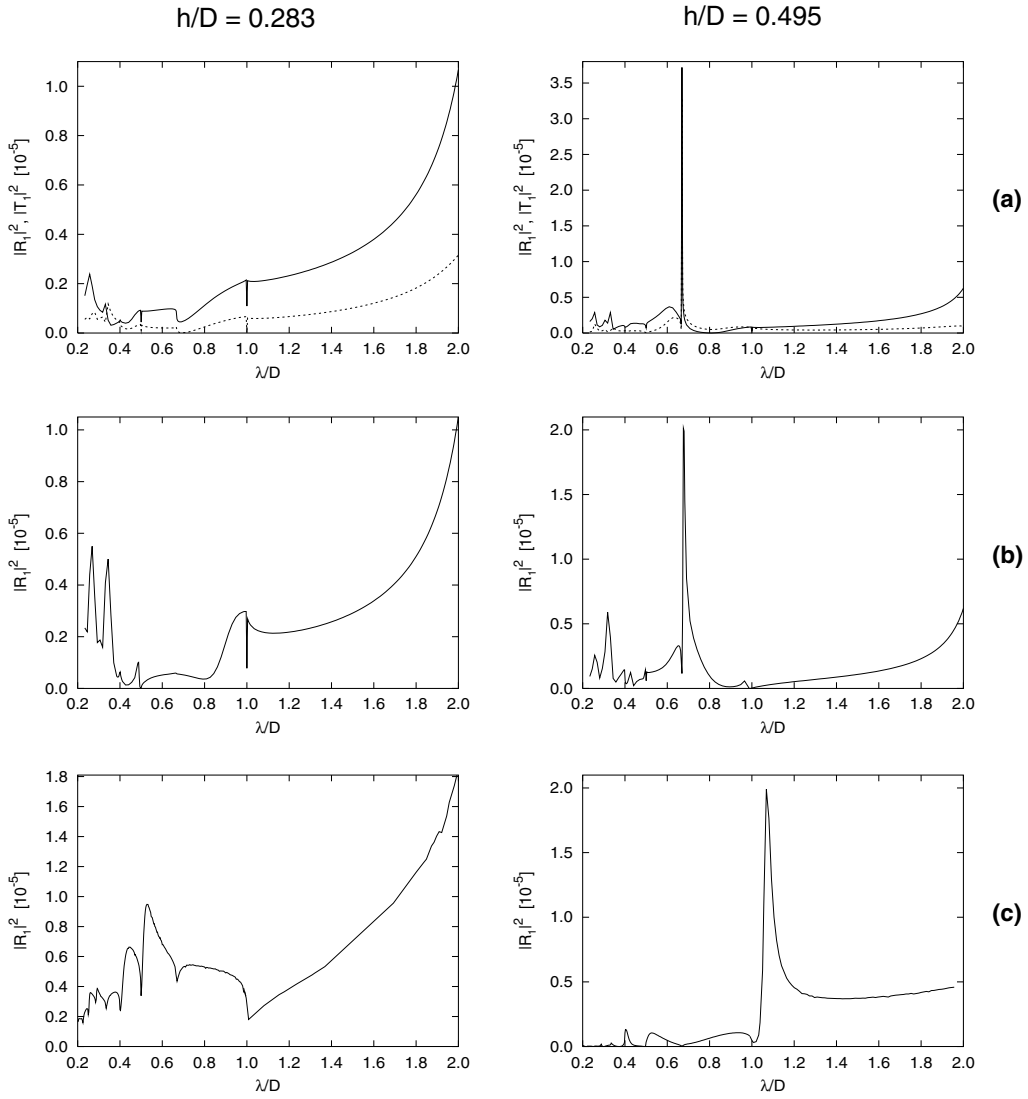


Fig. 6. Radiation factors (solid line) and transmission factors (dashed line) for a strip profile (a), a lamellar profile (b) and an échelette-type profile (c). Parameters of calculation: $a/D = 0.5$, $E = 855$ MeV. The aspect ratios $h/D$ correspond to the values of two échelette gratings with blaze angles 17.27°, respectively, 41.12° which were used in the experiment [19].

reader is referred to the books of Petit [33] or Hutley [34].

Secondly in the surface current approach the height $h$ of the grating strips is not taken into account. Apart from the technical aspect that the ridges for a strip grating separated by vacuum gaps must have a certain height the calculations in Fig. 3 show a strong influence of the radiation factors on $h$. Although the range of validity for the surface current model is restricted to shallow gratings [27] the comparison of Fig. 3(c) and (d) indicates that even shallow gratings still show a pronounced $h$ dependency.

Finally possibilities to use SP radiation for beam diagnostics are discussed. While SP based bunch length measurements might be a promising

approach the application for transverse beam imaging in the optical spectral region seems to fail because of the technical realization of the appropriate grating structure. For this purpose more detailed optimization studies are required which may result in an extension of the theoretical approach.

## Acknowledgements

The author would like to thank Dr. K. Wittenburg, DESY Hamburg (Germany), Prof. H. Backe and Dr. W. Lauth, Institut für Kernphysik, Universität Mainz (Germany) and Prof. A.P. Potylitsyn, Tomsk Polytechnic University (Russia) for stimulating discussions.

## References

[1] L. Wartski, S. Roland, J. Lasalle, M. Bolore, G. Filippi, J. Appl. Phys. 46 (1975) 3644.
[2] D.W. Rule, R.B. Fiorito, A.H. Lumpkin, R.B. Feldman, B.E. Carlsten, Nucl. Instr. and Meth. A 296 (1990) 739.
[3] M. Castellano, M. Ferrario, S. Kulinski, M. Minestrini, P. Patteri, F. Tazzioli, L. Catani, L. Gregorini, S. Tazzari, Nucl. Instr. and Meth. A 357 (1995) 231.
[4] X. Artru, M. Castellano, L. Catani, R. Chehab, D. Giove, K. Honkavaara, P. Patteri, M. Taurigna-Quere, A. Variola, L. Wartski, Nucl. Instr. and Meth. A 410 (1998) 148.
[5] M. Castellano, Nucl. Instr. and Meth. A 394 (1997) 275.
[6] R.B. Fiorito, D.W. Rule, Nucl. Instr. and Meth. B 173 (2001) 67.
[7] J. Urakawa et al., Nucl. Instr. and Meth. A 472 (2001) 309.
[8] A.P. Potylitsin, N.A. Potylitsyna, Russ. Phys. J. 43 (2000) 56.
[9] N. Potylitsyna-Kube, X. Artru, Nucl. Instr. and Meth. B 201 (2003) 172.
[10] P. Karataev, G. Naumenko, A. Potylitsyn, Nucl. Instr. and Meth. B 201 (2003) 133.
[11] P. Karataev, S. Araki, R. Hamatsu, H. Hayano, T. Hirose, T. Muto, G. Naumenko, A. Potylitsyn, J. Urakawa, Nucl. Instr. and Meth. B 201 (2003) 201.
[12] I.M. Frank, Izv. Akad. Nauk SSSR Ser. Fiz. 6 (1942) 3.
[13] S.J. Smith, E.M. Purcell, Phys. Rev. 92 (1953) 1069.
[14] M.C. Lampel, Nucl. Instr. and Meth. A 385 (1997) 19.
[15] D. Nguyen, Nucl. Instr. and Meth. A 393 (1997) 514.
[16] G. Doucas, M.F. Kimmitt, A. Doria, G.P. Gallerano, E. Giovenale, G. Messina, H.L. Andrews, J.H. Brownell, Phys. Rev. ST Accel. Beams 5 (2002) 072802.
[17] G. Doucas, M.F. Kimmitt, J.H. Brownell, S.R. Trotz, J.E. Walsh, Nucl. Instr. and Meth. A 474 (2001) 10.
[18] G. Kube, H. Backe, W. Lauth, H. Schöpe, in: Proc. Diag. Instrum. Part. Acc. Conf. DIPAC 2003, Mainz, 2003, p. 51.
[19] G. Kube et al., Phys. Rev. E 65 (2002) 056501.
[20] P.M. Van den Berg, J. Opt. Soc. Am. 63 (1973) 689.
[21] P.M. Van den Berg, J. Opt. Soc. Am. 63 (1973) 1588.
[22] P.M. Van den Berg, J. Opt. Soc. Am. 64 (1974) 325.
[23] J.P. Bachheimer, Phys. Rev. B 6 (1972) 2985.
[24] O. Haeberlé, P. Rullhusen, J.M. Salomé, N. Maene, Phys. Rev. E 49 (1994) 3340.
[25] A. Gover, P. Dvorkis, U. Elisha, J. Opt. Soc. Am. B 1 (1984) 723.
[26] M. Goldstein, J.E. Walsh, M.F. Kimmitt, J. Urata, C.L. Platt, Appl. Phys. Lett. 71 (1997) 452.
[27] J.H. Brownell, J. Walsh, G. Doucas, Phys. Rev. E 57 (1998) 1075.
[28] S.R. Trotz, J.H. Brownell, J.E. Walsh, G. Doucas, Phys. Rev. E 61 (2000) 7057.
[29] L.N. Deryugin, Radio Eng. Electron. Phys. (USSR) 15 (1960) 25.
[30] O. Haeberlé, Dissertation, Université Louis Pasteur, Strasbourg, 1994, unpublished.
[31] T. di Francia, Il Nuovo Ciment. 16 (1960) 61.
[32] D. Maystre, R. Petit, Opt. Commun. 5 (1972) 90.
[33] R. Petit (Ed.), Electromagnetic Theory of Gratings, Springer-Verlag, Berlin, 1980.
[34] M.C. Hutley, Diffraction Gratings, Academic Press London, New York, 1982.